Computational Materials Science 193 (2021) 110421

Contents lists available at ScienceDirect

Computational Materials Science

journal homepage: www.elsevier.com/locate/commatsci

Relaxation, crystal nucleation, kinetic spinodal and Kauzmann temperature in supercooled zinc selenide

Leila Separdar [a,*], José Pedro Rino [a], Edgar Dutra Zanotto [b]

[a] Department of Physics, Federal University of São Carlos, Via Washington Luís, km. 235, 13.565-905 São Carlos, SP, Brazil
[b] Department of Materials Engineering, Federal University of São Carlos, Via Washington Luís, km. 235, 13.565-905 São Carlos, SP, Brazil

ARTICLE INFO

Keywords:
Molecular dynamics
Nucleation
Relaxation
Kinetic spinodal
Kauzmann temperature
Supercooled liquid
ZnSe

ABSTRACT

Structural relaxation and crystallization are crucial phenomena in physics, chemistry, and materials science. A thorough study of their relationship could clarify some critical open questions. In this article, we focus on thermodynamic and kinetic properties: the Kauzmann temperature, T_K (where the excess entropy tends to zero), the kinetic spinodal temperature, T_{ks} (where the relaxation and crystal nucleation curves cross), and the glass transition temperature, T_g. We used zinc selenide (ZnSe) as a model system for which a reliable potential is available and obtained the self-diffusion coefficient, viscosity, critical nucleus birth times, relaxation times, entropy, T_g, T_{ks} and T_K by molecular dynamics (MD) simulations. We confirmed that the Stokes-Einstein equation breaks down in the moderate supercooled regime, impacting the relationships between the dynamic and thermodynamic properties. Two relaxation times were determined in the supercooled liquid (SCL) state: i) using the shear viscosity and the Maxwell equation, τ_η, and ii) from the self-intermediate scattering function and the Kohlrausch equation, τ_R. We found that in the whole supercooling regime, $\tau_\eta \ll \tau_R$ confirming two recent experimental studies for other substances. The nucleus birth times, τ_N, were also obtained for two system sizes. The $\tau_R(T)$ and $\tau_N(T)$ curves indeed crossover, confirming the existence of a kinetic spinodal temperature for this system. Hence, for temperatures somewhat above and below the T_{ks}, crystallization of the SCL could be affected by structural relaxation. Finally, our results demonstrate that if the Kauzmann temperature existed, it would be well below the T_{ks}. Hence, crystal nucleation intervenes on the cooling path, and SCL ZnSe *cannot* reach this temperature, thus averting the paradoxical entropic situation. These findings shed light on some central problems related to supercooled liquids.

1. Introduction

Due to its substantial scientific and technological relevance, understanding and describing the relaxation and crystallization mechanisms and kinetics of supercooled liquids (SCL) are relevant, fascinating and challenging. Structural relaxation is a key phenomenon that plays a significant role in vitrification and crystallization. Moreover, if a liquid is deeply supercooled without vitrifying or crystallizing, a particularly intriguing possibility is that it could reach the isentropic temperature, T_K, predicted by Kauzmann, at which the difference between the entropy of the SCL and its isochemical crystal (excess entropy) vanishes. Hence, for a temperature somewhat lower than T_K, the excess entropy would become negative and eventually reach zero above $T = 0K$, which would contradict the Third Law of thermodynamics. This conundrum is known as the Kauzmann paradox [1]. In this article, we are not advocating the existence of T_K; instead, we will test whether this temperature could be reached by an SCL before it crystallizes on the cooling path. Premature crystallization would avoid the paradoxical situation.

To properly understand the atomistic dynamics of a SCL, one must measure, theoretically calculate or simulate at least two characteristic times: one is related to the intrinsic atomic diffusivity that leads to the structural rearrangement of the supercooled liquid [2–5] and is called relaxation time, τ_R. The other characteristic time is the average period necessary to spontaneously form the first crystalline critical nucleus, the so-called nucleation time τ_N. According to the Classical Nucleation Theory, τ_N is controlled by the diffusion coefficient, D, and the thermodynamic barrier for crystallization, ΔG^*,

$$\tau_N = (A/D)exp\left(\frac{\Delta G^*}{k_B T}\right) \quad (1)$$

* Corresponding author.
E-mail address: separdar.leila@gmail.com (L. Separdar).

https://doi.org/10.1016/j.commatsci.2021.110421
Received 12 February 2021; Received in revised form 24 February 2021; Accepted 26 February 2021
Available online 18 March 2021

where A is the kinetic pre-factor [2] and k_B is Boltzmanns constant.

The race between these two characteristic times determines whether a supercooled liquid would relax before the birth of the first crystal nucleus or vice- versa [3,6]. When cooling down a liquid to any temperature between the equilibrium melting point, T_m, and the glass transition temperature, T_g, τ_N decreases, reaching a minimum (where the nucleation rate is maximum), and then increases for deeper supercoolings. This non-monotonic $\tau_N(T)$ relationship is explained by the classical nucleation/growth theory [2,7,8]. Crystallization occurs if $\tau_N < \tau_R$, otherwise the supercooled liquid can relax and even vitrify; i.e., become a glass. The temperature at which τ_N becomes equal to τ_R, is called the *kinetic spinodal* temperature, T_{ks}. One should note that the crossover temperature, T_{ks}, is *not* the classical thermodynamic spinodal, where the thermodynamic barrier for the liquid/crystal transformation vanishes. Due to its inherent complexity, the relationship between these two characteristic times has been scarcely investigated. To the best of our knowledge, this relation has only been studied experimentally for a few substances: the oxide glass-forming systems $Li_2O.2B_2O_3$ and $Li_2O.2SiO_2$ [6], and by computer simulations in pressurized SiO_2 [9], supercooled Ni [10], Cu [11], Cu_5Zr [12], Kob-Anderson (KA) binary Lennard-Jones mixture [13], Cu_xZr_{1-x} for a range of compositions from $x = 0.15$ to 0.645 [13], and more recently in BaS [14]. Simulation studies of Ni and BaS above the glass transition temperature, and an experimental study above and below the T_g for $Li_2O.2SiO_2$ and $Li_2O.2B_2O_3$, have indicated that T_{ks} is significantly *lower* than T_g. Hence crystallization of the SCL (above T_g) occurs *after* structural relaxation for these four substances. In the case of Cu and Cu_5Zr, T_{ks} is above T_g for the specific cooling rate studied; hence these supercooled liquids crystal nucleation starts *before* completion of the structural relaxation process. In the case of the supercooled liquid of a toy model glass former (Kob-Andersen model) [13] and for the model metallic glass former copper zirconium (Cu_xZr_{1-x}), $x = 0.15$ to 0.645 [13], these two characteristic times were evaluated above the glass transition temperature, however, T_{ks} was not reported. The common feature of all these materials is that crystallization takes place on the cooling path.

The microscopic mechanism of crystallization in above mentioned materials were related to dynamic heterogeneity in the SCLs, as mentioned in refs. [9–12], or to a series of discrete avalanche-like events characterized by regions composed of one species that are larger than the critical nucleus of that species. Nucleation in these regions is fast, apparently requiring little atomic rearrangement, as reported for the KA binary Lennard-Jones, Cu_xZr_{1-x} [13] and hard spheres at strong supercooling [15,16]. It should be stressed that, among all these studies, only in refs. [6,9] were the Kauzmann temperatures estimated and compared with the respective kinetic spinodal temperatures for three materials. Both studies have shown that T_{ks} is *higher* than T_K. Hence, for these three substances, crystallization intervenes on the cooling path and the paradoxical temperature T_K cannot be reached by the SCL.

These previous studies were quite revealing; however, some crucial open questions still remain: i) do all supercooled liquids and glasses ultimately nucleate (crystallize) in the deeply supercooled regime? To the best of our knowledge, only in the above mentioned seven materials ($Li_2O.2B_2O_3$, $Li_2O.2SiO_2$, pressurized SiO_2, Ni, Cu, Cu_5Zr, and BaS) the existence of the spinodal temperature has been investigated, and only three of them ($Li_2O.2B_2O_3$, $Li_2O.2SiO_2$, pressurized SiO_2) also estimated the Kauzmann temperatures. Hence further studies are needed to reach a universal description for the ultimate fate of SCLs. ii) Is $T_{ks} > T_K$ for all SCLs? By thoroughly testing another substance, we attempt to build up more knowledge on this particular issue. iii) A third related problem is the following: is it factual that the equilibrium shear viscosity controls the intrinsic structural relaxation process in SCL? This question is also extremely relevant because it is often assumed that structural relaxation can be calculated by the liquid viscosity (η = equilibrium shear viscosity) via the Maxwell equation,

$$\tau_\eta = \eta / G_\infty \tag{2}$$

where G_∞ is the infinite frequency shear modulus. In fact, in many experimental studies, e.g., [6], the equilibrium shear viscosity is used to calculate the relaxation times. Because τ_N and τ_R are (possibly) controlled by atomic self-diffusion and viscous flow, understanding the possible relation between these properties is also crucial. Later, we will show that two recent experimental works indicated that Eq. (2) is not a good predictor for structural relaxation for two different materials; hence, it would be relevant to test this concept with other substances and techniques, e.g., MD simulation.

For temperatures far above the glass transition temperature, homogeneous liquids normally obey the Stokes-Einstein equation (SE),

$$\frac{D\eta}{T} = constant. \tag{3}$$

The possible correlation between the existence of the kinetic spinodal temperature and the validity of the SE relation at deep supercoolings was investigated in [17]. It was argued that if the SE relation is assumed for the transport term of Eq. (1), the T_{ks} would not exist and the two-time scales would never cross. The SE breakdown is correlated with the dynamically heterogeneous nature of supercooled liquids and, by extension, with the fragility of most glass formers [12,18–21]. Another current question is the following: is it this breakdown that makes it possible for τ_N and τ_R to become comparable at sufficiently low temperatures?

In this study, we simulate and compare τ_N, τ_R and τ_η to investigate the possible existence of T_{ks} for another system, zinc selenide (ZnSe), and also compare T_{ks} with T_K. Finally, we aim to clarify another related open question, i.e., whether the structural relaxation kinetics can be described by the equilibrium shear viscosity. The substance chosen as a model for this study is ZnSe because we developed a reliable potential [22], which allows reliable determination of relaxation times, and have also shown that, in a relatively wide supercooling range, ZnSe spontaneously crystallizes in MD simulation time scales [23]. Hence, it also provides this opportunity to evaluate τ_N directly. In the next section, we explain the simulation details and the results obtained for the diffusion coefficient, D, viscosity, η, the average relaxation time, τ_R, nucleation time, τ_N, and excess entropy, S_{exc} , as a function of temperature. We then use these data and their extrapolated curves to find out the kinetic spinodal and Kauzmann temperatures and compare them. Then, in Section 3 we discuss the main results, and finally summarize them in the Conclusions section.

2. Simulation details and results

Our results are based on the molecular dynamics simulations of ZnSe with two different system sizes containing $17,576$ and $32,768$ Zn and Se atoms. Details about the potential used and simulation parameters are available in Refs. [22,23]. All simulations were performed by the LAMMPS package [24] in NpT and NVT ensembles. The timestep was $1.0fs$. The Nosé-Hoover thermostat and barostat were used to control the temperature and pressure. Periodic boundary conditions were applied in all directions.

The melting temperature was obtained through the two-phase coexistence method, resulting in $T_m = 1388K$ [23]. Fig. 1 shows the behavior of the atomic volume (V/N) as a function of temperature during heating/cooling process of the two system sizes for the cooling rate $1K/ps$. The red and green lines relate to systems containing $17,576$ and $32,768$ atoms, respectively. From this plot, one can estimate the glass transition temperature, T_g, of each system size by the intersection of linear fits to high and low temperature atomic volume data. T_g depends on the cooling rate applied. In Fig. 1 T_g is approximately $800 \pm 20K$. Doubling the size of the system just decreases it by 3%.

We also quantified the dynamical properties of the supercooled liquid by evaluating D, η, τ_R and τ_N for several temperatures from $1600K$ down to $900K$. The average nucleation time, τ_N, was calculated at three temperatures $T = 1000, 950, 900K$ because for the specific cooling rate

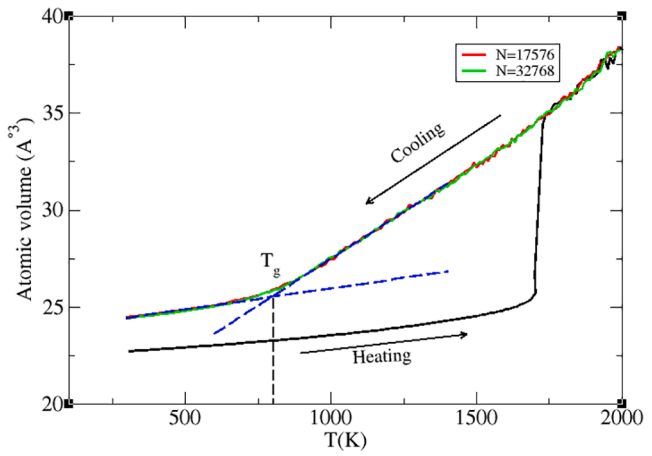

Fig. 1. Atomic volume of ZnSe as a function of the temperature during heating/cooling. The red and green lines relate to systems containing 17,576 and 32,768 atoms, respectively. Dashed lines are linear fits for high and low temperature atomic volume data. The vertical line marks T_g, the intersection between the linear fits.

used here, crystallization occurs spontaneously at $T < 1050K$, and can be measured on our computational time scale.

2.1. The diffusivity

One of the simplest quantities for describing the atomic dynamics is the translational diffusion coefficient, which can be obtained by a linear fit to a long-time regime of the mean-square displacements (MSD = $<r^2(t)>$) and using the Einstein relation $<r^2(t)> = 6Dt$. Fig. 2 presents the Arrhenius-type plot for calculated $D(T)$ values (from the slope of the simulated MSD plots at a long time), versus temperature in the range of $1000K < T < 1600K$ for both Zn and Se atoms. A fit to the data by the Arrhenius expression, $D = D_0 \exp(-\frac{E_A}{K_B T})$ gives the activation free energies $E_A = 0.60eV$ for Zn and $E_A = 0.73eV$ for Se. The pre-exponential factors are $D_0 = 53.9A^{\circ 2}/ps$ for Zn and $D_0 = 108.54A^{\circ 2}/ps$ for Se. Therefore, Zn is faster than Se. However, the Arrhenius expression cannot fit the temperature dependence of D_{Zn} and D_{Se} over the entire temperature range. This difference between the diffusivities of Zn and Se could cause dynamic heterogeneity, which is the reason for the breakdown of the SE relation (we will discuss this issue in the next section) and leads the SCL towards crystallization or vitrification. At T = 1050 K and 1000 K, some nucleation events were observed on the cooling path, and the diffusivity

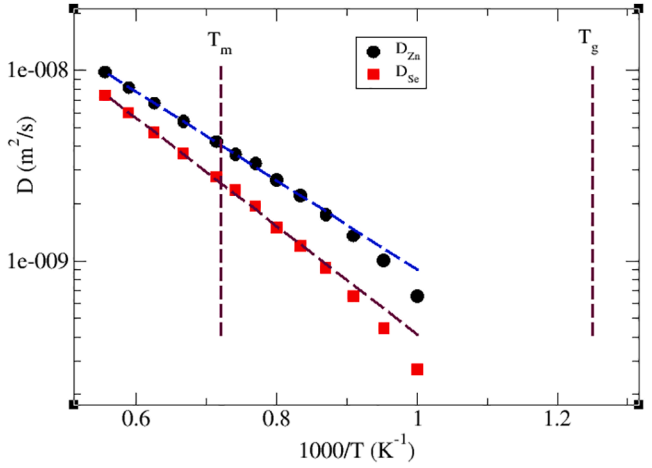

Fig. 2. Arrhenius plot of the simulated translational diffusion coefficient, $D(T)$, in ZnSe obtained from the MSD. Dashed lines are fits to an Arrhenius expression.

is smaller than predicted by extrapolation using the Arrhenius expression fitted at high temperature data. The average values of D_{Zn} and D_{Se} are used to analyze the validity of the SE relation. Doubling the system size in the simulation did not change the diffusivity values.

2.2. Viscosity

To obtain the shear viscosity, we used the Green-Kubo (GK) relation via the stress tensor correlation function;

$$\eta = \frac{V}{NK_BT}\int_0^\infty \langle p_{ij}(0)p_{ij}(t)\rangle dt, \tag{4}$$

where p_{ij} is the off-diagonal element of the pressure tensor, p_{xy}, p_{xz}, p_{yz}. V is the volume and N is the number of particles in the system. The shear viscosity is an average over all three off-diagonal terms $\eta = \frac{1}{3}\left(p_{xy}+p_{xz}+p_{yz},\right)$.

Fig. 3 shows a semi-log plot of viscosity as a function of inverse temperature in the range $1050K < T < 1800K$ (simulated data) and $625K < T < 1600K$ (extrapolated values). Each data point is averaged over five independent equilibrated systems. The error bars refer to the standard deviation. Calculation of the shear viscosity using the GK relation needs convergence of the integral of Eq. (4). This convergence is often an issue in supercooled liquids because the pressure-pressure correlation functions decay very slowly towards zero, especially at deep supercoolings. Hence, in this article we only report the viscosity values at temperatures for which convergence occurred (see Appendix for details).

Increasing the simulated system size did not change the viscosity significantly. We tested this possibility with the following box sizes: $L_x = L_y = L_z = 73.3A^\circ$ and $L_x = L_y = L_z = 90.3A^\circ$, which refer to systems comprising 17,576 and 32,768 atoms, respectively.

Several models describe the viscosity behavior. The most popular are the Vogel-Fulcher-Tamman (VFT) [25], the Avramov-Milchev (AM) [26] and the Mauro–Yue–Ellison–Gupta–Allan (MYEGA) equation [27]. The three models are described as follows:

$$\text{MYEGA}: log_{10}(\eta) = log_{10}(\eta_\infty) + \frac{A}{T}\exp\left(\frac{B}{T}\right), \tag{5}$$

$$\text{VFT}: log_{10}(\eta) = log_{10}(\eta_\infty) + \frac{A}{T-B}, \tag{6}$$

$$\text{AM}: log_{10}\eta(T) = log_{10}\eta_\infty + \left(\frac{A}{T}\right)^B, \tag{7}$$

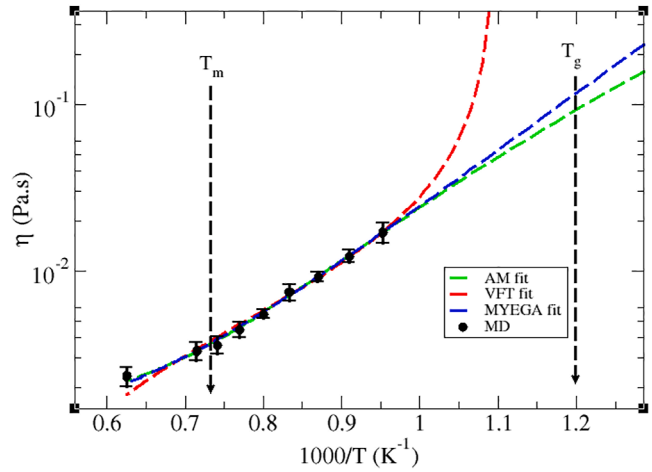

Fig. 3. Shear viscosity, η, as a function of inverse temperature. The simulated viscosity data were fitted and extrapolated to $T < T_g$ with the VFT equation (dashed red line), MYEGA equation (dashed blue line) and AM equation (dashed green line).

where A, B and η_∞ are adjustable parameters resulting from fitting to viscosity data. The differences among these three models were compared in Ref. [27]. It was shown that the VFT breaks down at low temperatures and over-predicts viscosity values [28,29], whereas the AM yields a divergence of configurational entropy in the high-temperature limit.

Among these, the MYEGA viscosity equation shows an improved description of the viscosity-temperature relationship based on the temperature dependence of configuration entropy both at high- and low-temperature regions. Here, we used the three models to describe the behavior of viscosity and the fits were shown in Fig. 3 with dashed lines and the values of fitting parameters are presented in Table 1. Although all three models describe the behavior of viscosity at high temperatures well, in the deep supercooling regime the extrapolated values of viscosity significantly differ. The differences were discussed in Ref. [30]. It was related to a systematic error of the AM model, and to the unphysical divergence of viscosity at low temperatures in the VFT model. Among them, the MYEGA model exhibits no such systematic error when performing both at the high- and low-temperature limits, which leads to the improved accuracy in performing low-temperature extrapolations [27]. Hence, we only use the MYEGA model in the next sections to describe the temperature dependence of relaxation times.

Fig. 4 shows the translational diffusion coefficient, D, calculated from the MSD versus T/η. It shows that the SE relation starts to break down soon below the melting point and does not hold in the supercooled regime probed here. The decoupling of the self-diffusion coefficient from viscosity is a manifestation of the heterogeneity in the dynamics of fragile liquids upon supercooling [18–21]. Indeed, when these liquids are cooled down towards T_g, local relaxation occurs at substantially different rates at different places within the liquid, i.e., the dynamics becomes spatially heterogeneous. This fragile nature of supercooled liquid ZnSe is also demonstrated by the breakdown in the temperature dependence of diffusivity. In the next section, we discuss the relaxation time in the supercooling regime.

2.3. Relaxation time

Structural relaxation refers to the liquid structure rearrangement until reaching the SCL state, which is metastable against the crystalline state. Direct microscopic observation of structural relaxation can be carried out by studying the behavior of the dynamic structure factor at its first maximum, or by its Fourier transformation, the intermediate scattering function, $F_s(q,t)$. The self-part of the intermediate scattering function (ISF) is defined as

$$F_s(q,t) = N_\alpha^{-1}\sum_{j=1}^{N_\alpha}\langle \exp(i\vec{q}\cdot\left[\vec{r}_j^{\,\alpha}(t) - \vec{r}_j^{\,\alpha}(0)\right]\rangle, \tag{8}$$

where the wave-vector, q, corresponds to the first sharp diffraction peak position, in our case, $q = 1.9\mathring{A}^{-1}$, N_α is the total number of Zn and Se particles in the simulation box, and $\vec{r}_j^{\,\alpha}(t)$ are the atomic positions of all j particles of species α. The ISF for Zn and Se atoms was calculated using the MD trajectories in the supercooled region at several temperatures both in the liquid and supercooled liquid regions for $900K < T < 1600K$. Fig. 5 (a) and (b) show the time dependency of the ISF for Zn and Se atoms, respectively. By decreasing the temperature, a plateau appears which is related to the time needed by particles to break out of the cage

Table 1
Fitting parameters of the simulated viscosity curve as a function of inverse temperature, Fig. 3.

Parameters	$log_{10}\eta_\infty$	A	B
MYEGA	0.001	0.02	7063.34
VFT	−0.002	2.66	911.47
AM	0.001	369.01	4.66

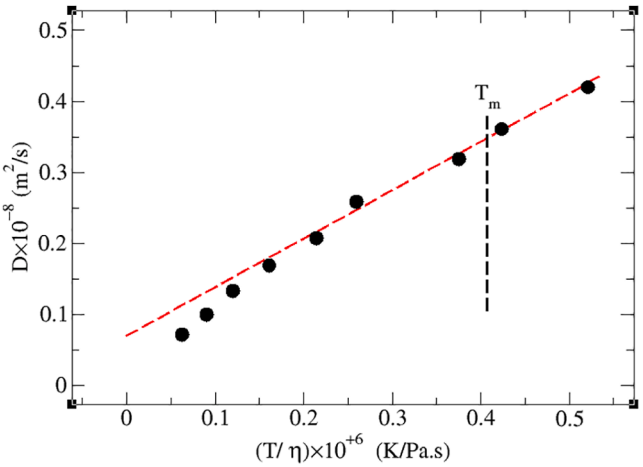

Fig. 4. Translational diffusion coefficient, $D(T)$, versus T/η. The red dashed line is a fit according to the SE relation, (Eq. (3)). The SE relation breaks down in the supercooled regime probed here.

created by neighboring particles. The Kohlrausch-Willian-Watts (KWW) function normally provides a good fit to the long-time behavior of the ISF [31] and is defined as

$$F_s(q,t) = F_s(q)\exp[-(\frac{t}{\tau_\alpha})^\beta] \tag{9}$$

where τ_α is the structural relaxation time, β is the stretched exponent;

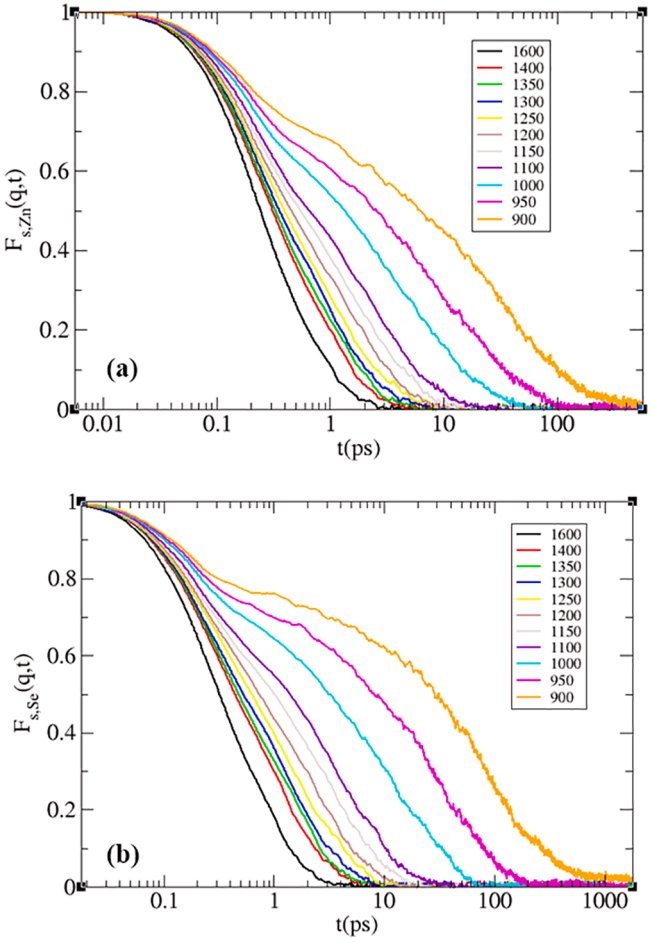

Fig. 5. Time dependence of the self-part of the intermediate-scattering function for (a) Zn, and (b) Se.

they are fitting parameters. Fig. 6 shows the calculated structural relaxation time as a function of temperature for both Zn and Se. For better statistics, five independent samples have been simulated at each temperature and the average of the structural relaxation times $< \tau_{\alpha,Zn} >$ and $< \tau_{\alpha,Se} >$ were calculated. The error bars are standard deviation. At high temperatures, τ_α changes almost linearly with temperature, whereas at lower temperatures it increases drastically and deviates from the linear behavior. The inset of Fig. 6 shows the temperature dependence of the stretched exponent, β. At higher temperatures for homogeneous liquids that are free of dynamic heterogeneity it approaches one. By decreasing the temperature, β decreases.

The average relaxation time, $\tau_R(T)$, is related to the average structural relaxation time as follows [32,33]:

$$\tau_R(T) = \frac{\tau_\alpha(T)}{\beta(T)}\Gamma\left(\frac{1}{\beta(T)}\right), \tag{10}$$

where Γ is the gamma function, $\tau_\alpha(T) = (< \tau_{\alpha,Zn} > + < \tau_{\alpha,Se} >)/2$ and $\beta(T) = (< \beta_{Zn} > + < \beta_{Se} >)/2$.

Fig. 7 shows the average relaxation time, τ_R, versus T/D. A fit to the data point according to the SE relation, $\frac{D\tau_R}{T} = constant$, shows that, by decreasing the temperature, the slope of τ_R as a function of inverse D changed significantly. This decoupling of the self-diffusion coefficient from the average relaxation times has also been found in computer simulations of other SCLs, such as hard-sphere [34], binary hard-sphere mixtures [35], a binary Lennard-Jones mixture [36], H_2O [37], SiO_2 [38], Ge [39] and $Al_{50}Ni_{20}$ [40].

2.4. Crystal nucleation time

We computed the *birth times*, τ_N, i.e., the average time needed for the first critical crystal nucleus to appear in the supercooled liquid at three temperatures $T = 1000, 950, 900K$ for two system sizes containing 17,576 and 32,768 atoms. The computations were based on detecting solid-like particles by calculating the Steinhardt bond-order parameter [41,42], $S_{ij} = \sum_{m=-6}^{m=+6} q_{6m}(i).q^*_{6m}(j)$, where $q_{6m}(i) = \frac{1}{N_b(i)}\sum_{j=1}^{N_b(i)} Y_{lm}(\vec{r}_{ij})$ is the Steinhardt parameter, $Y_{lm}(\vec{r}_{ij})$ are the spherical harmonics, $N_b(i)$ is the number of nearest neighbors of atom i, $\vec{r}_{ij}$ is the vector connecting atom i with its neighbors j. This procedure was carried out for 15 samples, and the reported birth times in Fig. 9 refers to the average over these 15 measurements. For each system size, the independent samples were allowed to evolve for $1ns$ and every $1000 timesteps = 1ps$, the atomic configurations were saved. At the end of the simulation, all configurations were analyzed and the number of solid-like atoms calculated via the q_6 order parameter. Fig. 8 shows the time evolution of the number of solid-like atoms for some selected samples at $T = 950K$. Table 2 shows the average τ_N and calculated steady-state nucleation rate $J_{ss}(T) = 1/\tau_N V$ at three temperatures for two system sizes. By increasing the system size at a given temperature, τ_N decreases in a way that the steady-state nucleation rates are almost the same for two different system sizes. As J_{ss} is a characteristic property of the system, one can calculate the average birth times for different system sizes, via $\tau_N = 1/(J_{ss}V)$. We calculated τ_N for a system of 3.7×10^{10} particles, which corresponds to a volume of $1\mu m^3$ (which approaches an experimental sample size). The temperature dependence of τ_N for all three system sizes are shown in Fig. 9. The birth times can be readily extrapolated to lower temperatures. We have determined the temperature dependence of the steady-state homogeneous nucleation rates, $J_{ss} = 1/\tau_N V$, using the nucleation rates that were fitted with the Classical Nucleation Theory (CNT) expression:

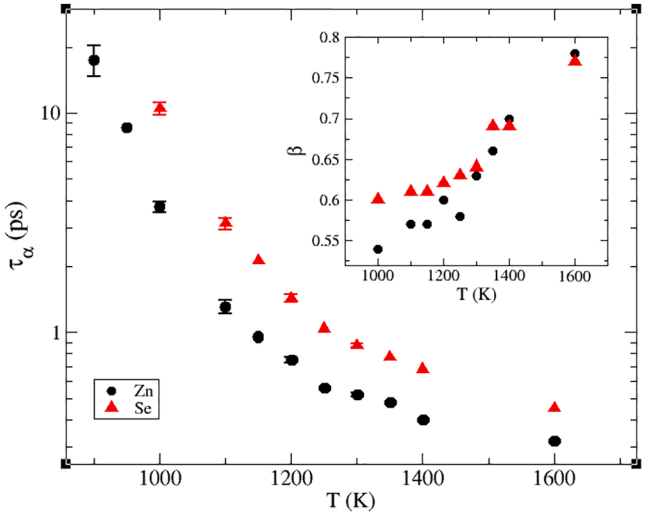

Fig. 6. Temperature dependence of the average structural relaxation time calculated from the self-intermediate scattering function via the KWW expression (Eq. (9)) for Zn and Se. Inset: Temperature dependence of the stretched exponent, β, calculated using the KWW expression.

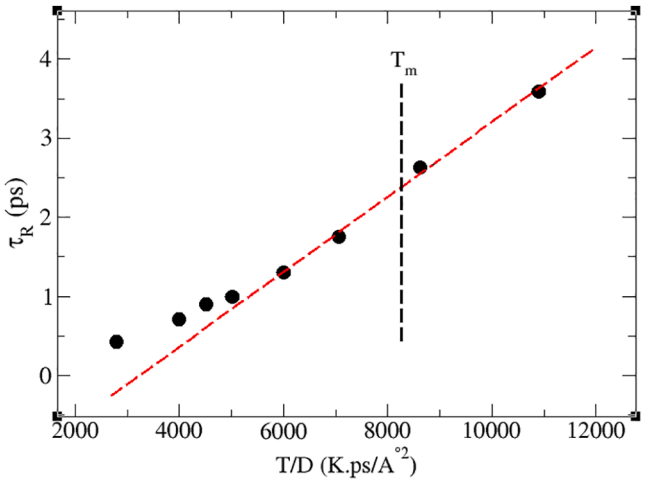

Fig. 7. Average relaxation time versus T/D for the temperature range $1000K < T < 1600K$. The line is a fit to the SE relation, $\frac{D\tau_R}{T} = constant$. At high temperatures, close or above T_m, the SE relation is obeyed, however by decreasing the temperature in the SCL state the SE relation is no longer valid.

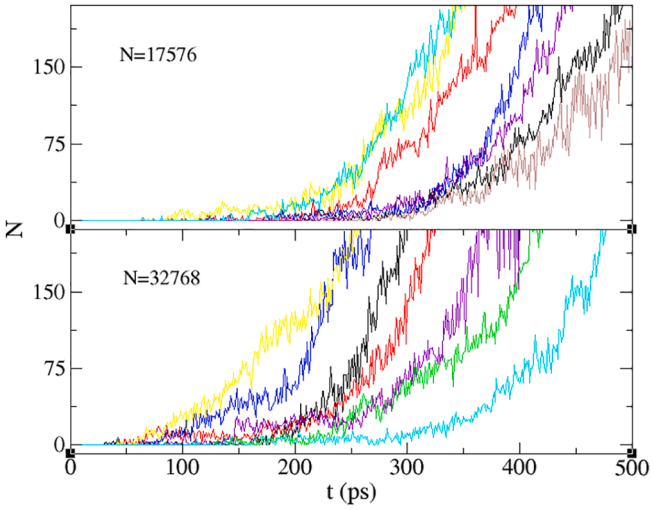

Fig. 8. Time evolution of the number, N, of solid-like atoms determined by calculating the q_6 order parameter at $T = 950K$ for two system sizes. Each line corresponds to a specific sample. To obtain the average birth time, τ_N, the onset times (when the number of atoms in the nucleus started to increase) were averaged over fifteen independent initial configurations.

Table 2
Values of τ_N and $J_{ss}(T)$ at three temperatures for two system sizes.

	N	$\tau_N(ps)$	$J_{ss}(ps^{-1}A^{\circ -3})$
$1000(K)$	17576	803.8	2.5×10^{-9}
	32768	740	1.5×10^{-9}
$950(K)$	17576	224.7	0.9×10^{-8}
	32768	168.3	0.7×10^{-8}
$900(K)$	17576	161.2	1.3×10^{-8}
	32768	78.8	1.4×10^{-8}

$$\frac{J_{ss}\sqrt{T}}{D} = Aexp\left(-\frac{B}{T\Delta G^{*2}}\right), \tag{11}$$

where A and B are fitting parameters, which are related to the pre-factor, the nucleus shape and the interfacial free energy, respectively. Therefore, by inverting $J_{ss}(T)$, the birth times ($\tau_N = 1/(J_{ss}V)$) could be extrapolated to lower temperatures. The extrapolation results are shown in Fig. 9 by blue, green and orange dashed lines.

We also calculated the relaxation times through the viscosity, τ_η, via Eq. (2), using $G_\infty = 30GPa$ of the crystal obtained from MD simulation. We assume that the infinite frequency shear modulus of the SCL is similar to that of the crystal. The results are shown in Fig. 9, where the temperature dependence of τ_N is compared to τ_R and τ_η. For shallow supercoolings, τ_N is longer than τ_R, indicating that relaxation occurs before nucleation. By decreasing the temperature, the gap between τ_N and τ_R decreases. For the largest simulated system size, $N = 32,768$, the two curves cross at $T_{ks} = 890 \pm 10K$. To find the kinetic spinodal temperature for other system sizes, we fitted τ_R with the MYEGA equation (Eq. (5)). The red arrows labeled 1, 2 and 3 show the crossover points, hence the predicted T_{ks} increases when the system size is increased. For all three systems, T_{ks} is above the glass transition temperature demonstrating that this particular system "crystalizes" (at least one critical nucleus is formed) before reaching the true glassy state. Hence, the measured T_g refers to the residual supercooled liquid, which already contains several critical crystalline nuclei formed on the cooling path. We estimated the critical cooling rate required to avoid nucleation by the relation [8]:

$$\frac{\Delta T}{\Delta t} = \frac{T_m - T_{nose}}{\tau_{nose}} \tag{12}$$

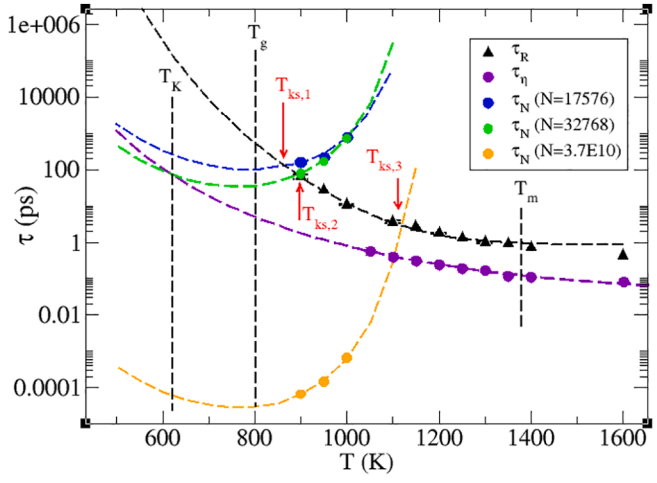

Fig. 9. Temperature dependence of nucleation birth times, τ_N, and average relaxation times estimated by fitting the intermediate scattering function, τ_R, and via viscosity, τ_η. The respective fittings and extrapolations of $\tau_R(T)$ and $\tau_\eta(T)$ with the MYEGA equation (Eq. (5)) and extrapolations of $\tau_N(T)$ with the CNT (Eq. (11)) are also shown. The vertical lines depict the glass transition, T_g, melting temperature, T_m, and the Kauzmann temperature, T_K. The red arrows demonstrate the crossover points of τ_N and τ_R (T_{ks}) for three system sizes.

τ_{nose} is time related to the T_{nose} (the minimum point in the time–temperature transformation curve). For systems containing 17,576 and 32,768 atoms, the critical cooling rates are 5.5 and 18.5 K/ps, respectively. Therefore, the cooling rate used in this study was $1K/ps$, which is lower than the two estimated critical cooling rates, hence we witnessed spontaneous nucleation already in the cooling procedure.

We found that τ_η is as much as an order of magnitude *smaller* than τ_R and converges to τ_N less rapidly than τ_N and τ_R, which is in accordance with the results of MD simulations of BaS [14] and two recent experimental works that have reached the same conclusion for other substances, a commercial glass and lead metasilicate glass [32,43], respectively. Hence, τ_η likely reflects the stress relaxation times, and only gives a lower bound for the structural relaxation times.

2.5. Kauzmann temperature

The Kauzmann temperature can be determined by computing the excess entropy, which is defined as the difference between the total entropy of the supercooled liquid and its isochemical crystal phase:

$$S_{exc}(T) = \frac{\Delta h_m}{T_m} + \int_{T_m}^{T} \frac{\Delta c_p(T')}{T'} dT' + \sum_i \frac{H_{c,i}}{T_{c,i}} \tag{13}$$

The temperature at which the excess entropy vanishes is the Kauzmann temperature. Here Δh_m is the enthalpy difference between liquid and crystal at the melting point. Δc_p is the difference between the specific heat of the supercooled liquid and crystal at constant pressure. The third term is the enthalpy of any polymorphic crystal phase transformation that might occur in the supercooling range. In the current system with $N = 17,576$ and $32,768$ atoms, no polymorphic crystalline phase was observed in the temperature range at which the S_{exc} was calculated ($T > 1050K$). From the slope of the time evolution of the respective enthalpies, we calculated the temperature dependency of the specific heat of the supercooled liquid and crystal. By inserting the $c_{p,liq}(T)$ and $c_{p,crystal}(T)$ into Eq. (13) and evaluating the integral, we calculated the excess entropy, which is shown in Fig. 10 by circles. Finally, by extrapolating the excess entropy to lower temperatures, it vanishes at $T_K = 630 \pm 15K$. This uncertainty in T_K was estimated by considering typical error of more or less 2% in T_m, Δh_m and Δc_p.

Hence, the estimated Kauzmann temperature is well below the kinetic spinodal temperature. For the oxide glass-forming systems $Li_2O.2B_2O_3$ and $Li_2O.2SiO_2$ [6], and in pressurized SiO_2 [9], the estimated Kauzmann temperatures are also lower than T_{ks}. Thus, our results for ZnSe corroborate those earlier studies for other substances and indicate that crystallization is indeed the SCLLs ultimate fate. Thus, the paradoxical temperature cannot be reached, at least for these four substances.

It is worth mentioning that, in doing the above estimate, we are not

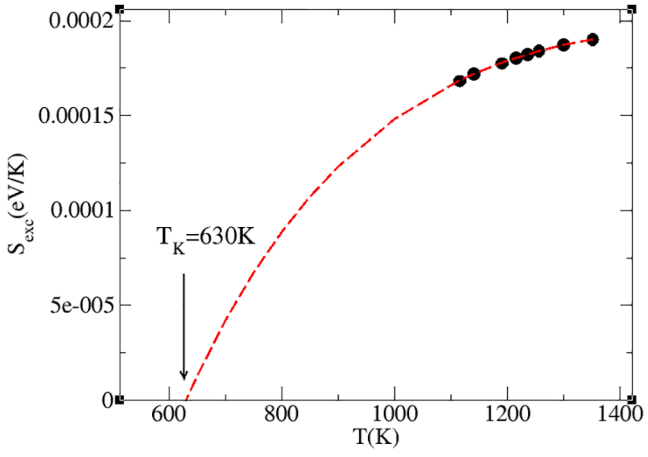

Fig. 10. Excess entropy of ZnSe as a function of temperature. The red dashed line displays the extrapolation of S_{exc} according to Eq. (13) down to T_K.

defending that the Kauzmann temperature is a physically meaningful quantity. It is likely an artifact of an extrapolation procedure that yields an apparent vanishing of excess entropy. Still, in reality, the excess entropy likely does not vanish on a longer time scale since other configurations can be explored compared to short simulations time scales [44]. The results of our simulations and calculations show that even if T_K could theoretically exist, it would never be reached because the SCL would crystallize at a higher temperature, $T_{ks} > T_K$.

3. Conclusions

In this work, we carried out extensive MD simulations of kinetic and thermodynamic properties of supercooled ZnSe, used as a model material. We found that the self-diffusion coefficient and viscosity of ZnSe are very similar in the liquid state and shallow supercoolings, but their proportionality breaks down at intermediate supercoolings. This disruption significantly affects the relationships between the properties of interest to this work.

The relaxation times obtained from the self-intermediate scattering function are *longer* than the values calculated from viscosity using the Maxwell relation. Hence, the relaxation times that are frequently calculated in this way underpredict the structural relaxation kinetics. This result confirms recent (2020–2021) MD simulations of BaS and experimental results for two other substances.

The kinetic spinodal temperature of ZnSe is significantly *higher* than the Kauzmann temperature. Hence, this supercooled liquid crystallizes before reaching T_K, thus averting the entropy catastrophe predicted by Kauzmann. Therefore, our findings corroborate the hypothesis of some (but not all) authors that the alleged paradox does not exist.

Finally, in the temperature range somewhat above and below the kinetic spinodal, crystal nucleation dynamics in the supercooled liquid should be affected by structural relaxation. This interference of relaxation on nucleation is *not* addressed by the current nucleation models but should be taken into account to analyze nucleation rates properly. This result corroborates recent theoretical predictions and experimental results for $Li_2O.2SiO_2$ [45,46] and $2Na_2O.1CaO.3SiO_2$ [47].

These findings shed light on crucial problems referring to supercooled liquids.

CRediT authorship contribution statement

Leila Separdar: Formal analysis, Investigation, Writing - original draft, Writing - review & editing, Visualization, Funding acquisition. **José Pedro Rino:** Conceptualization, Methodology, Validation, Writing - review & editing, Supervision, Project administration. **Edgar Dutra Zanotto:** Validation, Formal analysis, Writing - review & editing, Supervision, Project administration.

Declaration of Competing Interest

The authors declare that they have no known competing financial interests or personal relationships that could have appeared to influence the work reported in this paper.

Acknowledgments

We would like to thank CNPq, Brazil and the São Paulo Research Foundation, FAPESP, Brazil (contract CEPID # 2013/007793-6) for funding this work, and for a postdoctoral fellowship to LS (Grant # 2019/09499-4). The critical comments of Azat Tipeev, Daniel R. Cassar and Ricardo F. Lancelotti are greatly appreciated.

Data availability

All the data used in this article can be made available to any interested reader upon request to the authors.

Appendix

Pressure autocorrelation function

The accuracy of the Green-Kubo formulation for computing shear viscosity from equilibrium Molecular Dynamics simulations depends on the quality of the potential used to model the material, the simulation time, the number of particles, and how the correlations are accumulated. The Fig. A1 bellow shows the autocorrelation of the p_{xy} component of pressure tensor, $< p_{xy}(0)p_{xy}(t) >$ versus temperature for N = 17,576 particles for the temperature range $1000K < T < 1600K$. As the temperature decreases a longer time is needed for the autocorrelation of p_{xy} to approach zero. At $T = 1000K$, at which spontaneous crystallization occurs on the cooling path, this function does not converge to zero within the time frame available for our simulations.

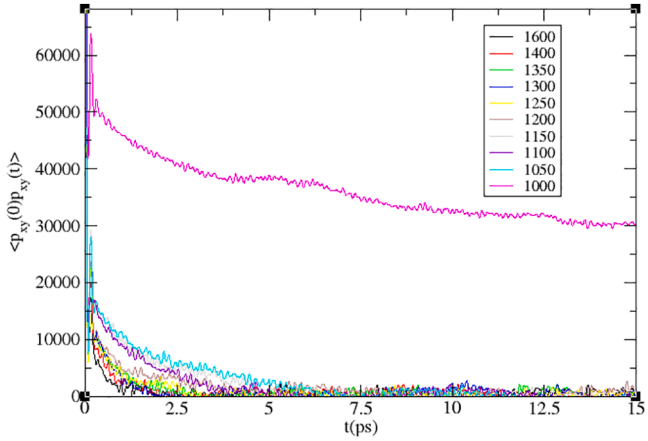

Fig. A1. Autocorrelation of the p_{xy} component of pressure tensor, $< p_{xy}(0)p_{xy}(t) >$ versus temperature for N = 17,576 particles for the temperature range $1000K < T < 1600K$.

References

[1] W. Kauzmann, The Nature of the Glassy State and the Behavior of Liquids at Low Temperatures. Chem. Rev. 43 (2) (1948) 219–256, https://doi.org/10.1021/cr60135a002.

[2] P.G. Debenedetti, Metastable liquids concepts and principles, Princeton University, Princeton, NJ, 1996.

[3] C.A. Angell, Formation of glasses from liquids and biopolymers, Science 267 (5206) (1995) 1924–1935, https://doi.org/10.1126/science:267.5206.1924.

[4] M.D. Ediger, C.A. Angell, S.R. Nagel, Supercooled liquids and glasses, J. Phys. Chem. 100 (31) (1996) 13200–13212, https://doi.org/10.1021/jp953538d.

[5] P.G. Debenedetti, F.H. Stillinger, Supercooled liquids and the glass transition, Nature 410 (6825) (2001) 259–267, https://doi.org/10.1038/35065704.

[6] E.D. Zanotto, D.R. Cassar, The race within supercooled liquids-Relaxation versus crystallization, J. Chem. Phys. 149 (2) (2018) 024503–024513, https://doi.org/10.1063/1.5034091.

[7] D. Turnbull, Under what conditions can a glass be formed? Contemp. Phys. 10 (5) (1969) 473–488, https://doi.org/10.1080/00107516908204405.

[8] D.R. Uhlmann, A kinetic treatment of glass formation, J. Non-Cryst. Solids 7 (4) (1972) 337–348, https://doi.org/10.1016/0022-3093(72)90269-4.

[9] I. Saika-Voivod, R.K. Bowles, P.H. Poole, Crystal nucleation in a supercooled liquid with glassy dynamics, Phys. Rev. Lett. 103 (22) (2009) 225701–225705, https://doi.org/10.1103/PhysRevLett.103.225701.

[10] Y. Zhang, L.i. Wang, W. Wang, Thermodynamic, dynamic and structural relaxation in supercooled liquid and glassy Ni below the critical temperature, J. Phys.: Condens. Matter 19 (19) (2007) 196106–196119, https://doi.org/10.1088/0953-8984/19/19/196106.

[11] H. Pang, Z.H. Jin, K. Lu, Relaxation, nucleation, and glass transition in supercooled liquid Cu, Phys. Rev. B 67 (9) (2003) 094113–094121, https://doi.org/10.1103/PhysRevB.67.094113.

[12] F. Puosi, A. Pasturel, Nucleation kinetics in a supercooled metallic glass former, Acta Materialia 174 (2019) 387–397, https://doi.org/10.1016/j.actamat.2019.05.057.

[13] T.S. Ingebrigtsen, J.C. Dyre, Th.B. Schrøder, C.P. Royall, Crystallization instability in glass-forming mixtures, Phys. Rev. X 9 (2019) 031016–031027, https://doi.org/10.1103/PhysRevX.9.031016.

[14] J.P. Rino, S.C.C. Prado, E.D. Zanotto, The race between relaxation and nucleation in supercooled liquid and glassy BaS: A Molecular Dynamics study, J. Comp. Mater. Sci. (2021) 110417–110424, https://doi.org/10.1016/j.commatsci.2021.110417.

[15] E. Sanz, C. Valeriani, E. Zaccarelli, W.C.K. Poon, M.E. Cates, P.N. Pusey, Avalanches mediate crystallization in a hard-sphere glass, Proc. Natl. Acad. Sci. 111 (1) (2014) 75–80, https://doi.org/10.1073/pnas.1308338110.

[16] T. Yanagishima, J. Russo, H. Tanaka, Common mechanism of thermodynamic and mechanical origin for ageing and crystallization of glasses, Nat. Commun. 8 (1) (2017) 15954–15964, https://doi.org/10.1038/ncomms15954.

[17] H. Tanaka, Possible resolution of the Kauzmann paradox in supercooled liquids, Phys. Rev. E 68 (1) (2003) 011505–011513, https://doi.org/10.1103/PhysRevE.68.011505.

[18] H. Sillescu, Heterogeneity at the glass transition: a review, J. Non-Cryst. Solids 243 (2–3) (1999) 81–108, https://doi.org/10.1016/S0022-3093(98)00831-X.

[19] M.D.S. Ediger, Spatially heterogeneous dynamics in supercooled liquids, Annu. Rev. Phys. Chem. 51 (2000) 99–128, https://doi.org/10.1146/annurev.physchem.51.1.99.

[20] M.M. Hurley, P. Harrowell, Kinetic structure of a two-dimensional liquid, Phys. Rev. E 52 (2) (1995) 1694–1698, https://doi.org/10.1103/PhysRevE.52.1694.

[21] M.K. Mapes, S.F. Swallen, M.D. Ediger, Self-diffusion of supercooled o-Terphenyl near the glass transition temperature, J. Phys. Chem. B 110 (2006) 1507–1511, https://doi.org/10.1021/jp0555955.

[22] S.C.C. Prado, J.P. Rino, An interaction potential for zinc selenide: a molecular dynamics study, J. Appl. Phys. 129 (2021) 055104, https://doi.org/10.1063/5.0033224.

[23] L. Separdar, J.P. Rino, E.D. Zanotto, Molecular dynamics simulations of spontaneous and seeded nucleation and theoretical calculations for zinc selenide, Comput. Mater. Sci. 187 (2021) 110124–110134, https://doi.org/10.1016/j.commatsci.2020.110124.

[24] S. Plimpton, Fast parallel algorithms for short-range molecular dynamics, J. Comput. Phys. 117 (1) (1995) 1–19, https://doi.org/10.1006/jcph.1995.1039.

[25] G.S. Fulcher, Analysis of recent measurements of the viscosity of glasses, J. Am. Ceram. Soc. 8 (6) (1925) 339–355, https://doi.org/10.1111/j.1151-2916.1925.tb16731.x.

[26] G. Adam, J.H. Gibbs, On the temperature dependence of cooperative relaxation properties in glass-forming liquids, J. Chem. Phys. 43 (1) (1965) 139–146, https://doi.org/10.1063/1.1696442.

[27] J.C. Mauro, Y. Yue, A.J. Ellison, P.K. Gupta, D.C. Allan, Viscosity of glass-forming liquids, Proc. Natl. Acad. Sci. 106 (47) (2009) 19780–19784, https://doi.org/10.1073/pnas.0911705106.

[28] G.W. Scherer, Editorial Comments on a Paper by Gordon S. Fulcher, J. Am. Ceram. Soc. 75 (5) (1992) 1060–1062, https://doi.org/10.1111/j.1151-2916.1992.tb05537.x.

[29] W.T. Laughlin, D.R. Uhlmann, Viscous flow in simple organic liquids, J. Phys. Chem. 76 (16) (1972) 2317–2325, https://doi.org/10.1021/j100660a023.

[30] Q. Zheng, J.C. Mauro, Viscosity of glass-forming systems, J. Am. Ceram. Soc. 100 (1) (2017) 6–25, https://doi.org/10.1111/jace.14678.

[31] S. Sastry, P.G. Debenedetti, F.H. Stillinger, Signatures of distinct dynamical regimes in the energy landscape of a glass-forming liquid, Nature 393 (6685) (1998) 554–557, https://doi.org/10.1038/31189.

[32] R.F. Lancelotti, O. Peitl, D.R. Cassar, M. Nalin, E.D. Zanotto, Is the structural relaxation of glasses controlled by equilibrium shear viscosity? J. Am. Ceram. Soc. 104 (2021) 2066–2076, https://doi.org/10.1111/jace.17622.

[33] K. Doss, C.J. Wilkinson, Y.J. Yang, K.H. Lee, L.P. Huang, J.C. Mauro, Maxwell relaxation time for nonexponential alpha-relaxation phenomena in glassy systems, J. Am. Ceram. Soc. 103 (6) (2020) 3590–3599, https://doi.org/10.1111/jace.17051.

[34] S.K. Kumar, G. Szamel, J.F. Douglas, Nature of the breakdown in the Stokes-Einstein relationship in a hard sphere fluid, J. Chem. Phys. 124 (21) (2006) 214501–214507, https://doi.org/10.1063/1.2192769.

[35] G. Foffi, W. Götze, F. Sciortino, P. Tartaglia, Th. Voigtmann, α-relaxation processes in binary hard-sphere mixtures, Phys. Rev. E 69 (1) (2004) 011505–011522, https://doi.org/10.1103/PhysRevE.69.011505.

[36] W. Kob, H.C. Andersen, Scaling behavior in the β-relaxation regime of a supercooled Lennard-Jones mixture, Phys. Rev. Lett. 73 (1994) 1376–1380, https://doi.org/10.1103/PhysRevLett.73.1376.

[37] F.W. Starr, F. Sciortino, H.E. Stanley, Dynamics of simulated water under pressure, Phys. Rev. E 60 (6) (1999) 6757–6768, https://doi.org/10.1103/PhysRevE.60.6757.

[38] J. Horbach, W. Kob, Relaxation dynamics of a viscous silica melt: The intermediate scattering functions, Phys. Rev. E 64 (2001) 041503–041517, https://doi.org/10.1103/PhysRevE.64.041503.

[39] M. Hawlitzky, J. Horbach, S. Ispas, M. Krack, K. Binder, Comparative classical and '*ab initio*' molecular dynamics study of molten and glassy germanium dioxide, J. Phys. Condens. Matter 20 (2008) 285106–285122.

[40] K. Das Subir, J. Horbach, Th. Voigtmann, Structural relaxation in a binary metallic melt: Molecular dynamics computer simulation of undercooled $Al_{80}Ni_{20}$, Phys. Rev. B 78 (2008) 064208–064221, https://doi.org/10.1103/PhysRevB.78.064208.

[41] P.J. Steinhardt, D.R. Nelson, M. Ronchetti, Bond-orientational order in liquids and glasses, Phys. Rev. B 28 (2) (1983) 784–805, https://doi.org/10.1103/PhysRevB.28.784.

[42] P.R. ten Wolde, D. Frenkel, Homogeneous nucleation and the Ostwald step rule, Chem. Phys. 1 (1999) 2191–2196, https://doi.org/10.1039/A809346F.

[43] K. Doss, C.J. Wilkinson, Y.J. Yang, K.H. Lee, L.P. Huang, J.C. Mauro, Maxwell relaxation time for nonexponential alpha-relaxation phenomena in glassy systems, J. Am. Ceram. Soc. 103 (2020) 3590–3599, https://doi.org/10.1111/jace.17051.

[44] J.C. Mauro, Through a glass, darkly: dispelling three common misconceptions in glass science, Int. J. Appl. Glass Sci. 2 (4) (2011) 245–261, https://doi.org/10.1111/j.2041-1294.2011.00069.x.

[45] J.W.P. Schmelzer, T.V. Tropin, V.M. Fokin, A.S. Abyzov, E.D. Zanotto, Effects of glass transition and structural relaxation on crystal nucleation: theoretical description and model analysis, Entropy 22 (2020) 1–36, https://doi.org/10.3390/e22101098.

[46] V.M. Fokin, A.S. Abyzov, N.S. Yuritsyn, J.W.P. Schmelzer, E.D. Zanotto, Effect of structural relaxation on crystal nucleation in glasses, Acta Materialia 203 (2021) 116472–116485, https://doi.org/10.1016/j.actamat.2020.11.014.

[47] L.R. Rodrigues, A.S. Abyzov, V.M. Fokin, E.D. Zanotto, Effect of structural relaxation on crystal nucleation in a soda-lime-silica glass, J. Am. Ceram. Soc. (2021), https://doi.org/10.1111/jace.17765.